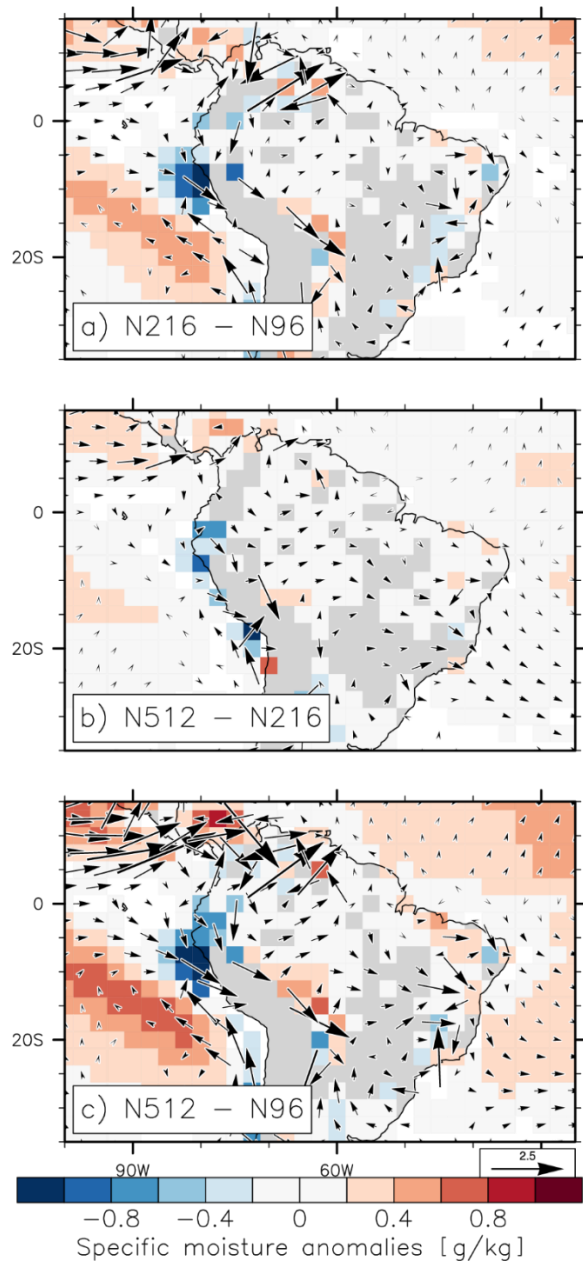


# **Supplementary material for “Role of atmospheric horizontal resolution in simulating tropical and subtropical South American precipitation in HadGEM3-GC31”**

Paul-Arthur Monerie<sup>1</sup>, Amulya Chevuturi<sup>1</sup>, Peter Cook<sup>1</sup>, Nick Klingaman<sup>1</sup>, Christopher E. Holloway<sup>2</sup>

<sup>1</sup> Department of Meteorology, National Centre for Atmospheric Science (NCAS), University of Reading, Reading, UK

<sup>2</sup> Department of Meteorology, University of Reading, Reading, UK



**Figure S1:** Ensemble-mean difference in annual mean surface specific humidity ( $\text{g.kg}^{-1}$ ) and 850 hPa wind ( $\text{m.s}^{-1}$ ), for (a) N216-N96, (b) N512-N216 and (c) N512-N96.

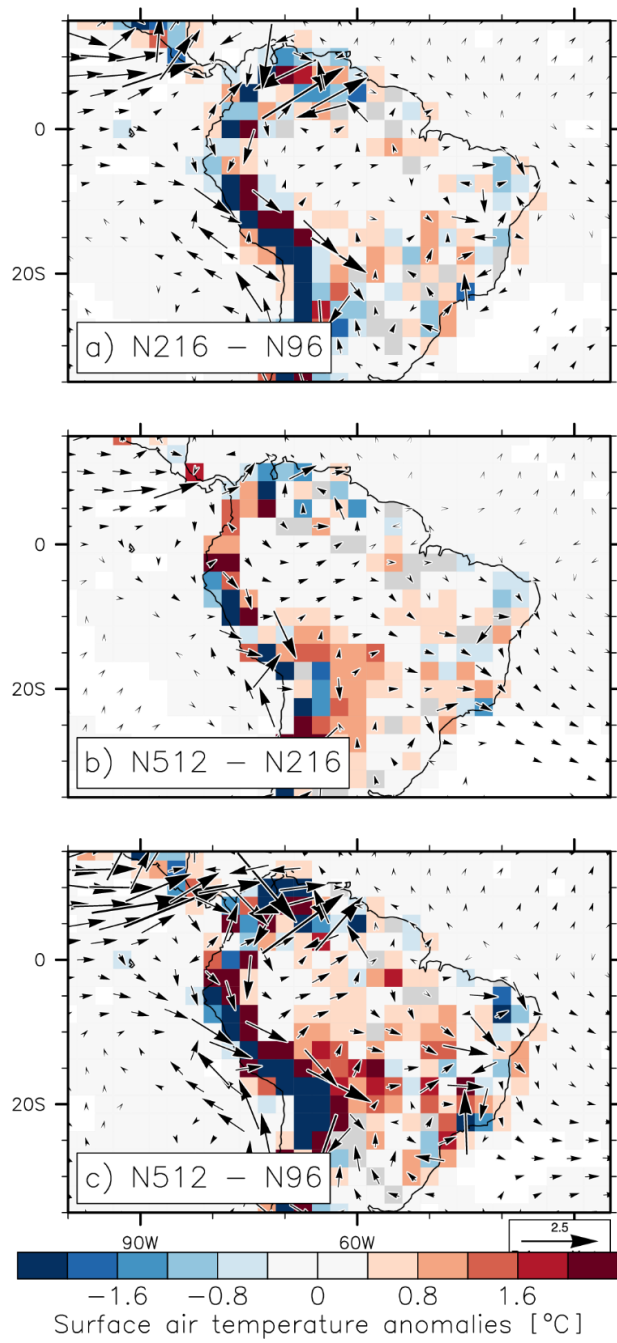


**Figure S2:** Ensemble-mean difference in annual mean surface air temperature (°C) and 850 hPa wind (m.s<sup>-1</sup>), for (a) N216-N96, (b) N512-N216 and (c) N512-N96.

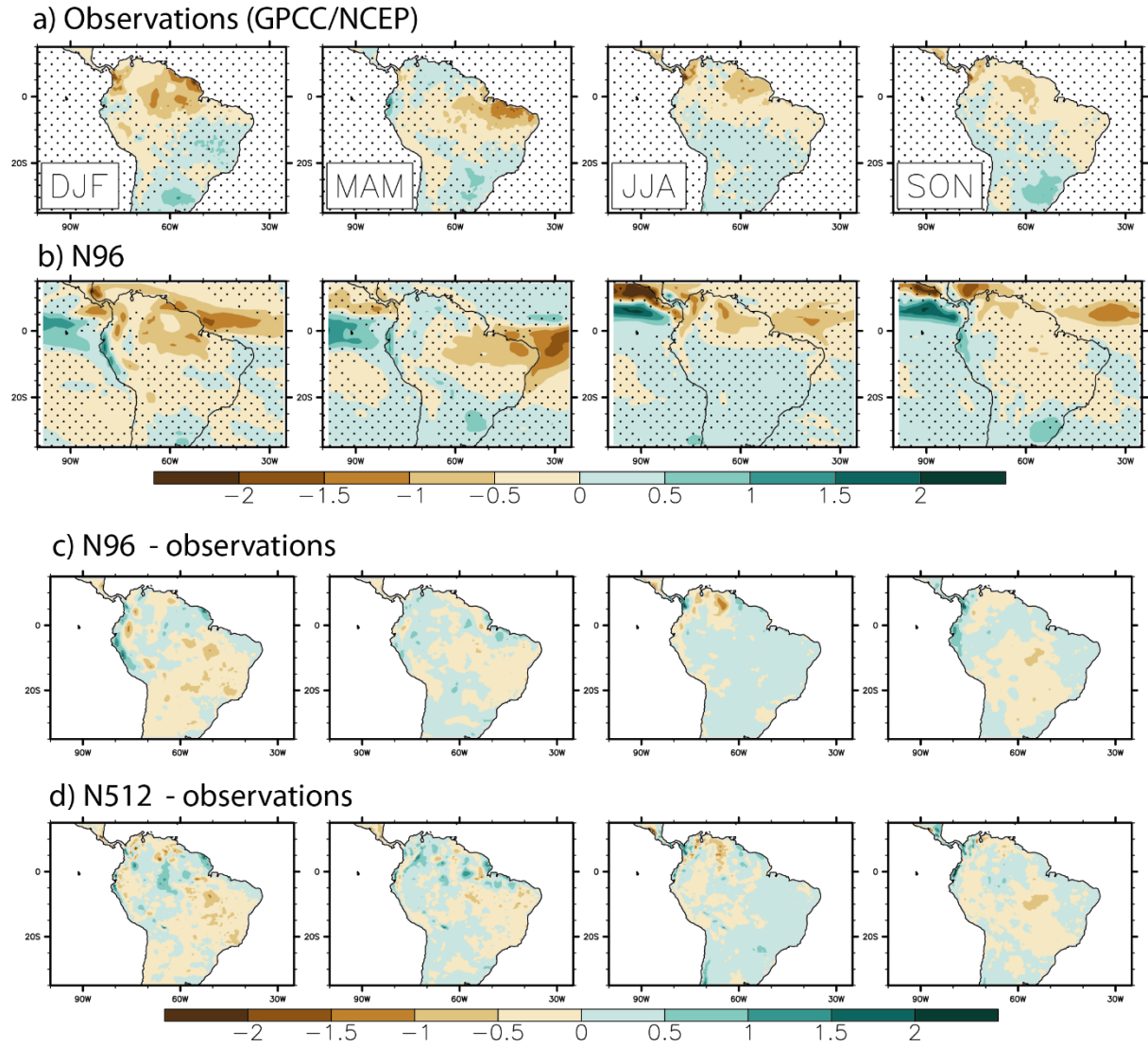


**Figure S3:** Precipitation regressed onto the EN3.4 index ( $\text{mm.day}^{-1}.\text{C}^{-1}$ ) with (a) observations (GPCC for precipitation and NCEP for temperature), (b) N96. Stippling is added when regression is not significant, using a Student's t-test and a 95% confidence level. Difference between (c) N96 and observations (i.e. (b)-(a)) and (d) N512 and observations.

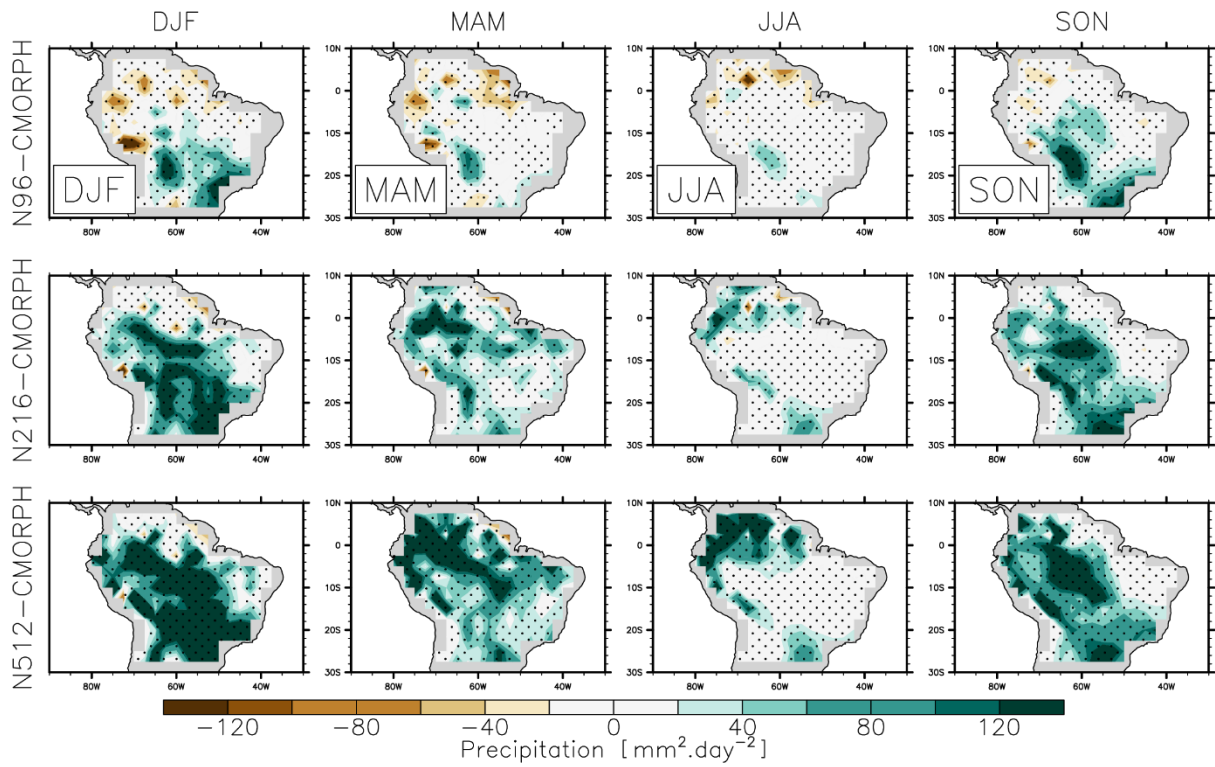


**Figure S4:** Bias in daily precipitation variance (mm<sup>2</sup>.day<sup>-2</sup>) in (top row) N96, (middle row) N216 and (bottom row) N512, with regard to CMORPH. Results are given for the DJF, MAM, JJA and SON seasons, over the 1998-2014 period. Stippling indicates that differences are significant according to an f-test and a 95% confidence level.

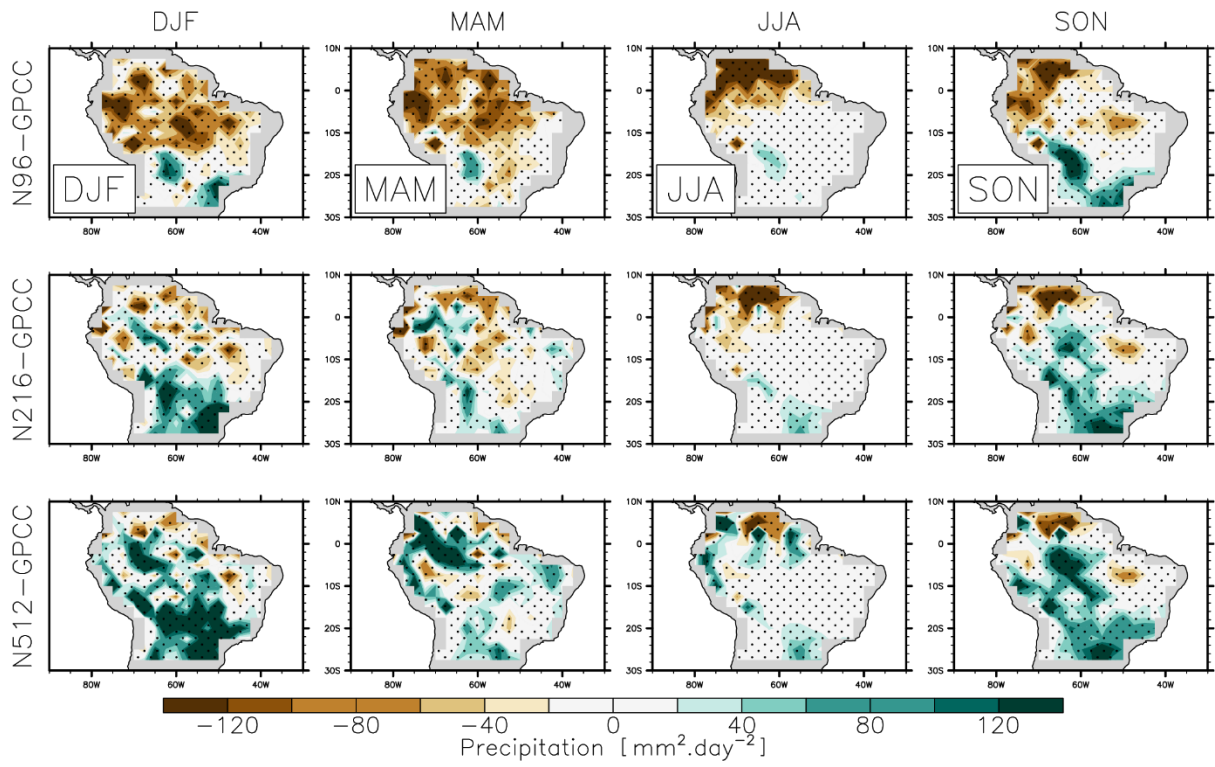


**Figure S5:** Bias in daily precipitation variance (mm<sup>2</sup>.day<sup>-2</sup>) in (top row) N96, (middle row) N216 and (bottom row) N512, with regard to GPCC. Results are given for the DJF, MAM, JJA and SON seasons, over the 1998-2014 period. Stippling indicates that differences are significant according to an f-test and a 95% confidence level.

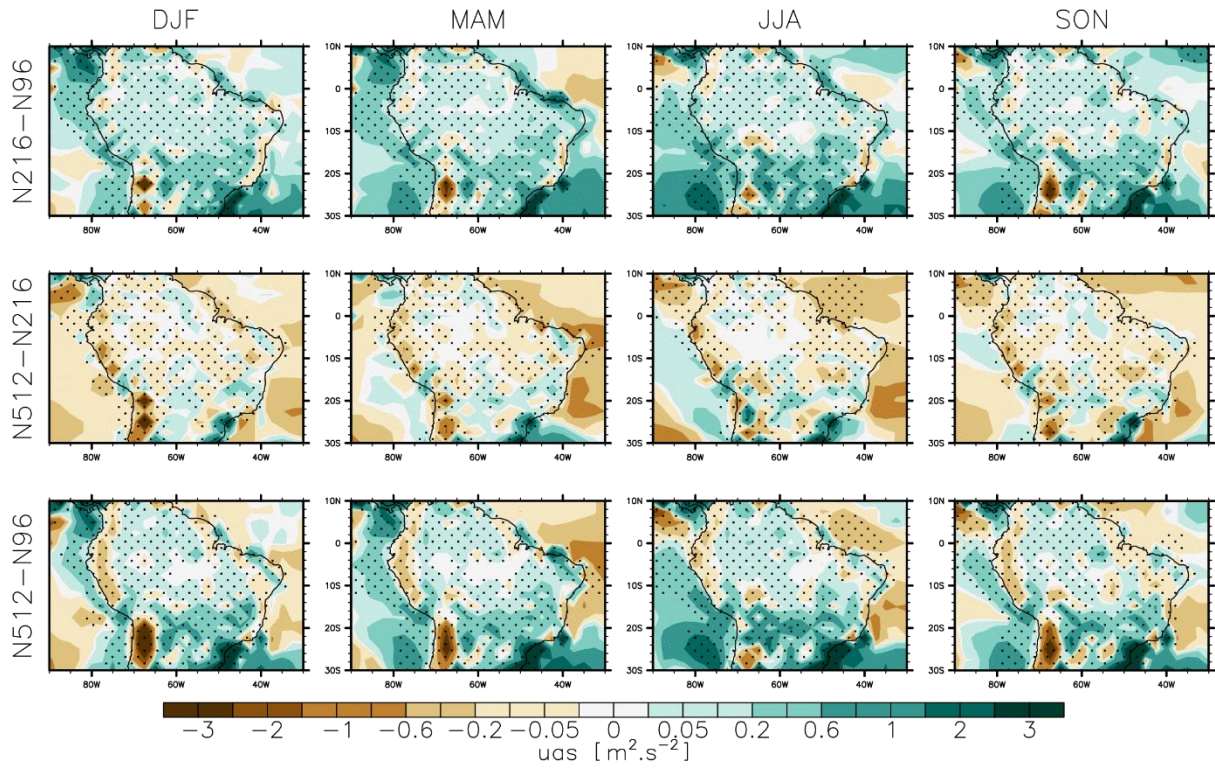


**Figure S6:** Ensemble-mean difference in surface zonal wind daily variance ( $m^2.s^{-2}$ ), for (top row) N216-N96, (middle row) N512-N216 and (bottom row) N512-N96. Results are given for the DJF, MAM, JJA and SON seasons, over the 1998-2014 period. Stippling indicates that differences are significant according to an f-test and a 95% confidence level.



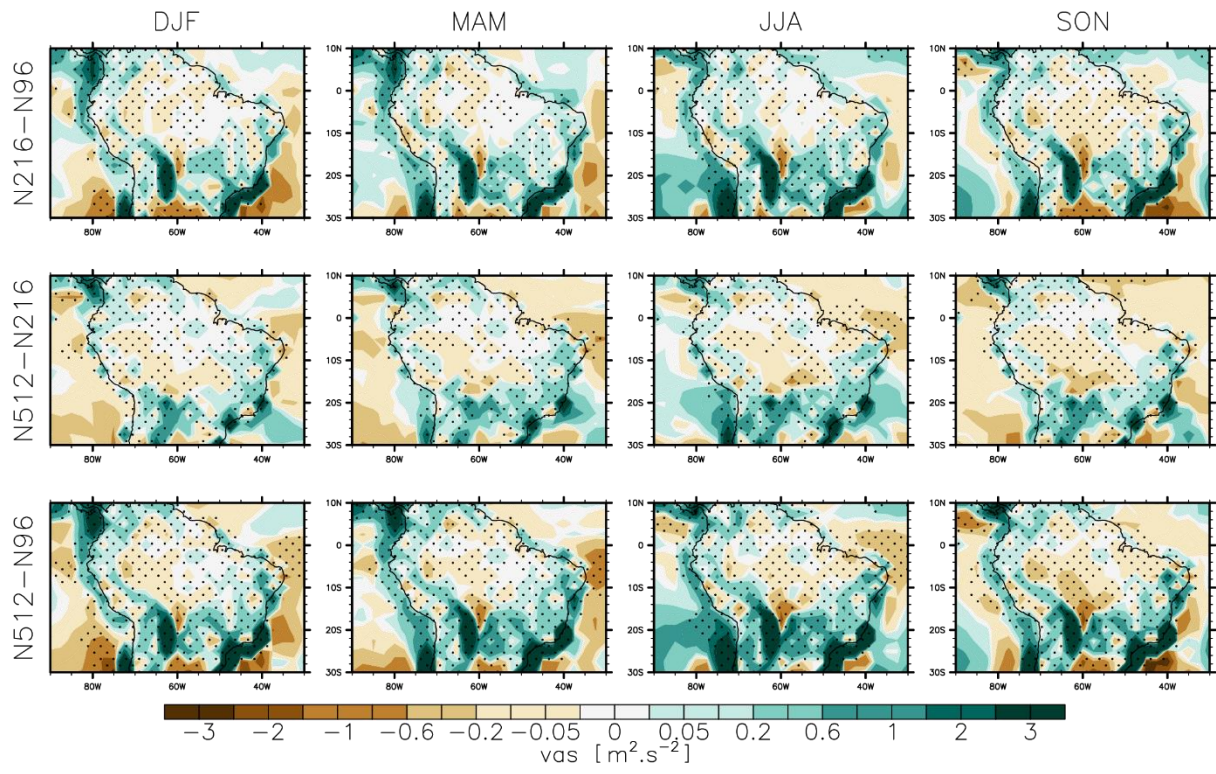


**Figure S7:** As in Figure S6 but for surface meridional wind.



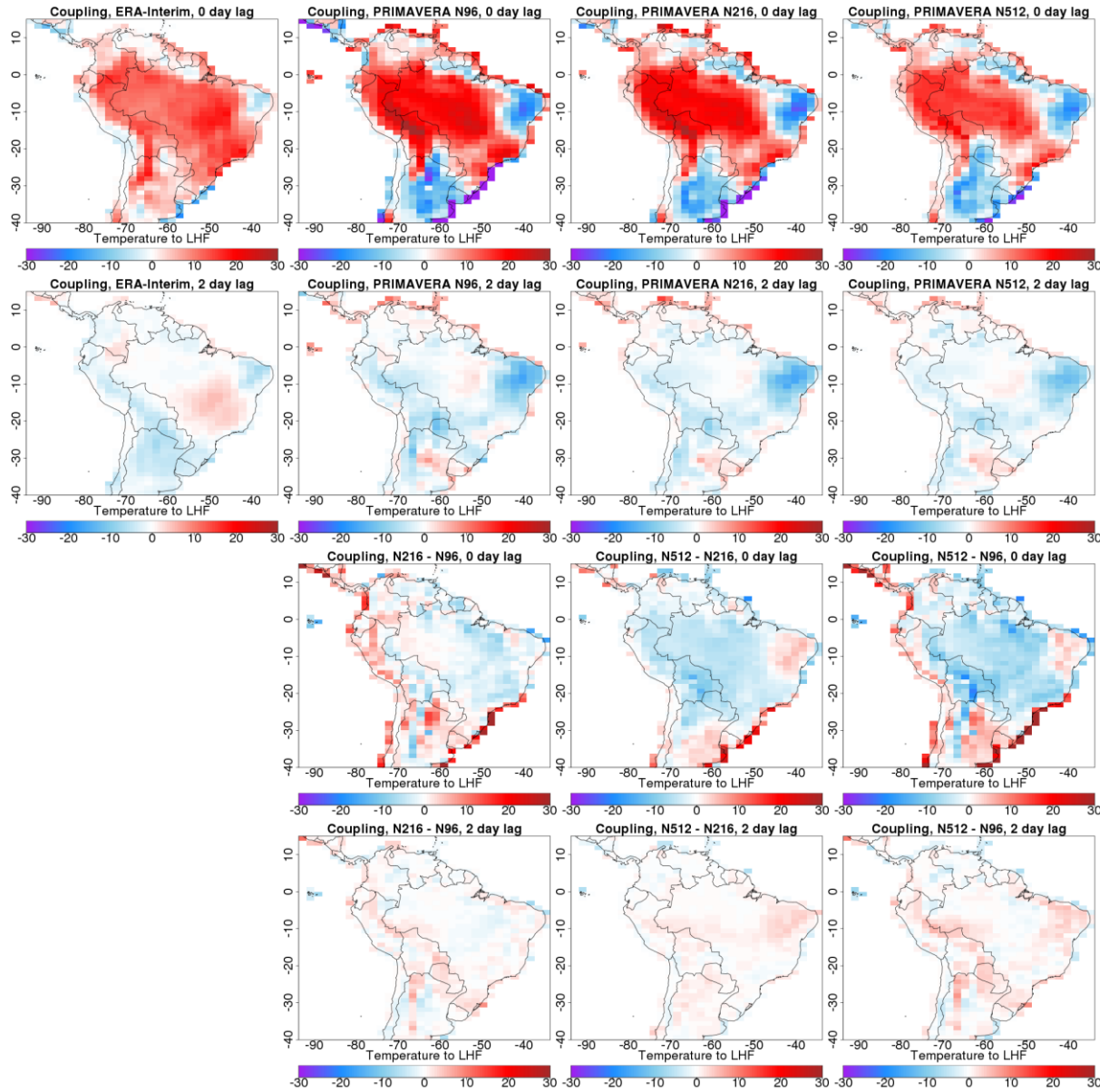


**Figure S8:** Coupling strength ( $r_{a,b}\sigma_b$ ) between daily temperature and latent heat flux during the southern summer wet season (DJF). Daily data from PRIMAVERA model ensembles (1950-2014) at 3 resolutions, and ERA-Interim reanalysis (1979-2014). Showing the results from ERA-Interim, differences between PRIMAVERA and ERA-Interim results, and differences between PRIMAVERA results at different resolutions, for 0 time lags and 2 day time lags (the soil situation 2 days after precipitation).

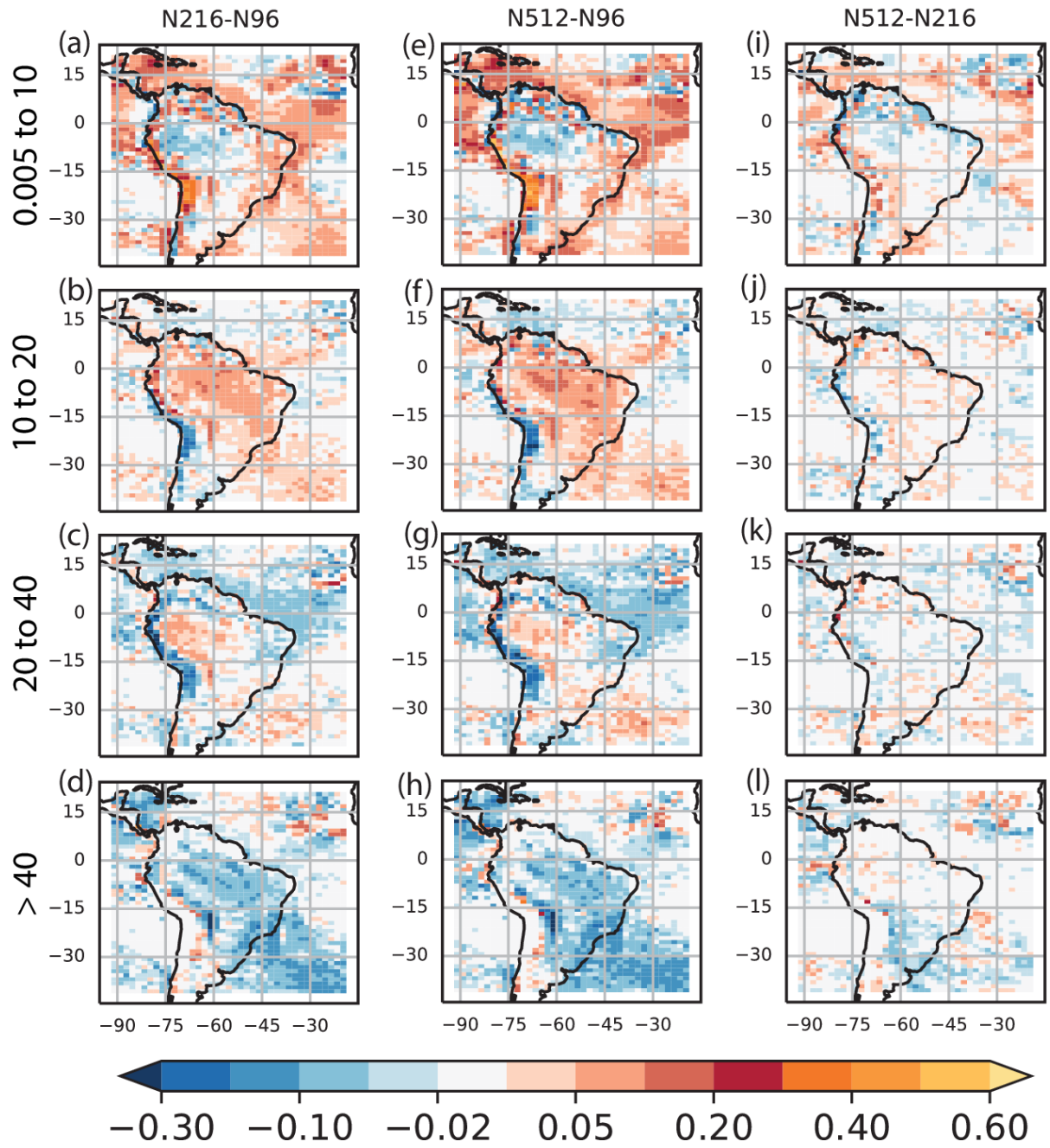


**Figure S9:** Differences in the fractional contribution to the total precipitation rate from ranges of intensity bins shown in the labels above each pane between N216 and N96 (a-d). The four ranges of intensity bins are (a) 0.005 to 10 mm/day, (b) 10 to 20 mm/day, (c) 20 to 40 mm/day and (d) >40 mm/day. Same as for N96-CMORPH but for N512 and N96 (e-h) and N512 and N216 (i-l).

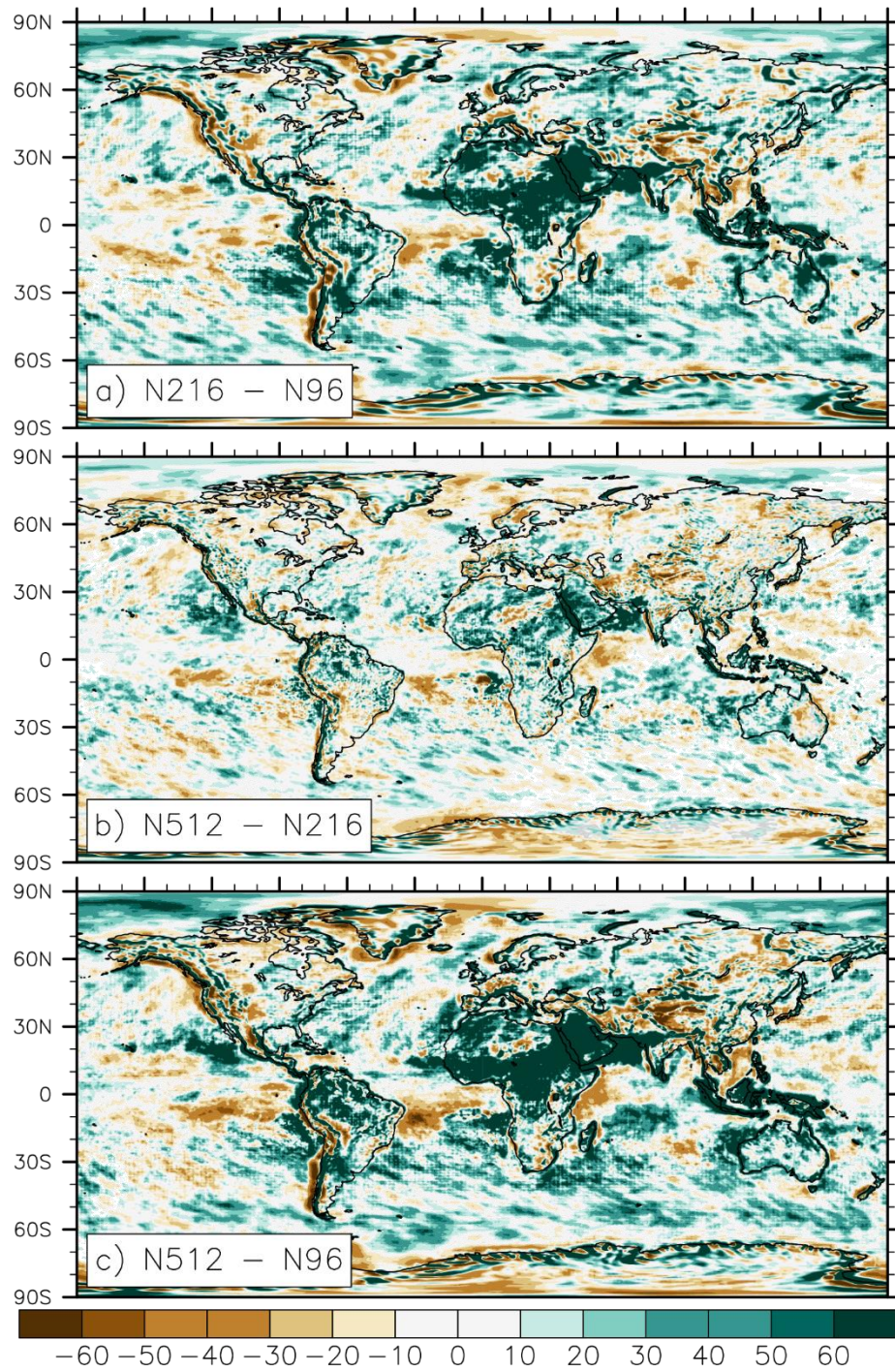


**Figure S10:** Ensemble-mean difference in annual mean precipitation variance (in %) for (a) N216-N96, (b) N512-N216 and (c) N512-N96.